ACCSCIENCE PUBLISHING

International Journal of Bioprinting

RESEARCH ARTICLE

3D-printed scaffolds with controlled-releasing compounds for ectopic activation of dormant ovarian follicles

Yali Yang[1†], Huashan Zhao[1†], Mingming Wu[2†], Lei Ge[1,3], Meiyue Wang[1], Feifei Du[1], Zhonglin Xiao[1,4], Li Xue[1,3], Pinpin Wang[2,3], Jie Chen[1], Tianxia Xiao[1], Pei-Gen Ren[1*], Changshun Ruan[2*], and Jian V. Zhang[1,5,6*]

[1]Shenzhen Key Laboratory of Metabolic Health, Center for Energy Metabolism and Reproduction, Shenzhen Institutes of Advanced Technology, Chinese Academy of Sciences, Shenzhen, Guangdong, China

[2]Center for Human Tissues and Organ Degeneration, Shenzhen Institutes of Advanced Technology, Chinese Academy of Sciences, Shenzhen, Guangdong, China

[3]University of Chinese Academy of Sciences, Beijing, China

[4]Faculty of Data Science, City University of Macau, Macau, China

[5]Faculty of Pharmaceutical Sciences, Shenzhen University of Advanced Technology, Shenzhen, Guangdong, China

[6]Sino-European Center of Biomedicine and Health, Shenzhen, Guangdong, China

[†]These authors contributed equally to this work.

***Corresponding authors:**
Pei-Gen Ren
(pg.ren@siat.ac.cn)

Changshun Ruan
(cs.ruan@siat.ac.cn)

Jian V. Zhang
(jian.zhang@siat.ac.cn)

Citation: Yang Y, Zhao H, Wu M, et al. 3D-printed scaffolds with controlled-releasing compounds for ectopic activation of dormant ovarian follicles. *Int J Bioprint*. 2025;11(1):246-258. doi: 10.36922/ijb.4941

Received: September 24, 2024
Revised: October 22, 2024
Accepted: October 30, 2024
Published Online: October 30, 2024

Copyright: © 2024 Author(s). This is an Open Access article distributed under the terms of the Creative Commons Attribution License, permitting distribution, and reproduction in any medium, provided the original work is properly cited.

Publisher's Note: AccScience Publishing remains neutral with regard to jurisdictional claims in published maps and institutional affiliations.

Abstract

Throughout a woman's reproductive life, hundreds of functioning follicles are activated for development, while thousands of dormant follicles remain in the ovaries. *In vitro* dormant follicle activation is an effective clinical strategy for women with fertility needs facing ovarian dysfunction. However, *in vivo* dormant follicle activation remains a challenge due to difficulties such as delivering stimulators to local sites. Here, we developed a compound-preloaded microporous scaffold by combining three-dimensional (3D) printing techniques with pharmacological activators to support and stimulate the activation and development of primordial follicles. The gelatin/alginate composite scaffolds exhibited exceptional mechanical properties and biological compatibility, effectively supporting the survival of ovarian granulosa cells for more than 7 days, which is essential for oocyte development. Furthermore, the ovarian tissue scaffold complex successfully survived after transplantation under the mouse kidney capsule, demonstrating its excellent biocompatibility. After pre-mixing widely used clinical activators into the bioink, the scaffold could gradually release the mixture of compounds, effectively activating primordial follicles. By transplanting the ovary–scaffold complex containing activators into the mouse abdominal subcutaneous pocket, dormant follicles could be activated subcutaneously and developed into growing follicles. The number of growing follicles is approximately three times higher compared to the group without activators. In conclusion, by integrating biomaterials, activators, and 3D printing technology, we have developed 3D-printed biological scaffolds that can ectopically support primordial follicle activation and development *in vivo*. This novel approach could provide a promising strategy for treating ovarian insufficiency and endocrine disorders in the clinic, without the need for *in situ* ovarian tissue grafting.

Keywords: 3D printing; Scaffold; Dormant ovarian follicles; Activation; Transplantation

1. Introduction

Ovarian dysfunction leads to female cycle disorders, menopause, and infertility.[1,2] To effectively address these issues, it is vital to have growing follicles available in the ovaries. Throughout a woman's reproductive years, only a limited number of primordial follicles are recruited and activated, leaving many dormant follicles in the ovaries. However, it remains a significant challenge to directly and effectively activate these dormant follicles *in vivo*.[3,4]

With the development of biomaterials and tissue engineering, using bioengineering to restore fertility has also gradually become a promising research avenue. Some research teams have used biocompatible materials and follicular cells to develop bioengineered ovaries.[5–9] It has been reported that ovarian tissues or oocytes wrapped in biocompatible materials can successfully produce healthy offspring,[10,11] suggesting that functional follicles can survive and grow in biocompatible material-printed grafts. The availability of functional follicles highly depends on the formation of a spherical structure composed of oocytes, surrounding granulosa cells, and theca cells, as well as indispensable angiogenesis, thereby establishing tissue-specific microenvironments.[12] However, biomaterials cannot provide sufficient space for the development of the follicles.

Since the invention of 3D printing by Chuck Hull in 1983, 3D printing technology has been widely used in the medical field, among which, 3D-bioprinted organs provide great convenience for clinical surgery, drug testing, and disease research. Meanwhile, 3D printing technology has been successfully applied to creating human organs such as liver, heart, and kidney.[13] However, its application in reproductive biology is still in its infancy, and restoring fertility through 3D-printed ovarian strategies is an exciting area of research.[14–19] Studies have demonstrated that mouse follicles can grow and ovulate successfully in 3D-printed porous scaffolds,[20] recover ovarian function *in vivo*, and even produce healthy offspring through natural mating.[17] However, these follicles are typically at advanced stages of development, such as preantral or antral follicles. For patients with undeveloped ovarian follicles, the scaffolds cannot help restore hormone levels or fertility. Therefore, a combination of the 3D-printed scaffold and primordial follicle activation, whether by activating follicles *in vitro* before transplantation, or by using the scaffold's slow-release properties for *in vivo* activation, holds significant research value for restoring hormone levels and fertility in patients with undeveloped follicles.

The selection of biomaterials for bioprinting is crucial to ensure the functionality of ovarian tissue. Gelatin is a water-soluble protein extracted from collagen, which is a main component of the extracellular matrix. Among various biomaterials, it is well-known for its excellent biocompatibility and biodegradability. After being chemically modified with methacryloyl, gelatin-methacryloyl (Gel-MA) can be easily solidified into a firm hydrogel under ultraviolet (UV) irradiation, making it a popular biomaterial as the printing ink.[21] Sodium alginate (Alg), a natural polysaccharide, is widely used in chemistry, biology, medicine, and food industries due to its film-forming, biodegradable, and biocompatible properties. These characteristics make it an ideal material for 3D bioprinting.[22]

In this study, we developed a 3D-printed porous scaffold using Alg and Gel-MA, leveraging their easy printing and molding characteristics, and incorporated stimulators to promote ectopic primordial follicle activation and growth. This Alg/Gel-based scaffold, featuring dual-crosslinking networks formed through ionic interactions between Alg and chemical crosslinking of Gel-MA, exhibits significantly improved mechanical properties. In addition, the activators were pre-mixed with the biomaterial, enabling the gradual release of the activators and the subsequent activation of primordial follicles after *in vivo* transplantation. Furthermore, our findings indicate that the 3D-printed scaffold containing activators can effectively support the ectopic activation of primordial follicles and subsequent development into growing follicles within the abdominal cavity of mice. This approach provides a promising direction for the clinical application of artificial ovaries and serves as a potential method for the clinical treatment of ovarian dysfunction and endocrine disorders.

2. Materials and methods

2.1. Materials

The main materials used in this study included gelatin from porcine skin (type A, reagent grade; Sigma-Aldrich, United States of America [USA]), MA (94%; Heowns Biochemical Technology Company, China), Alg (low viscosity; Sigma-Aldrich, USA), propranolol (PRO; BML-ST405-0005; Enzo Life Sciences, America), phosphatidic acid (PA; AvantiPolar Lipids, America), and a UV-light crosslinker (XL-1000 UV Crosslinker; Spectronics Corporation, USA).

2.2. Animals

All animal experiments were approved and performed in accordance with the guidelines of the Institutional

Animal Care and Use Committee of Shenzhen Institutes of Advanced Technology, Chinese Academy of Sciences. C57BL/6 mice were purchased from Beijing Vital River Laboratory Animal Technology Co., Ltd. (China) and maintained in our specific pathogen free-level animal facility. Green fluorescent protein (GFP)-reporting mice were purchased from the Nanjing Biomedical Research Institute of Nanjing University.

2.3. Bioink preparation and 3D printing

An appropriate amount (20 wt.%) of GelMA with 3 wt.% UV initiator 2-hydroxy-2-methylpropiophenone was dissolved in distilled water in a 60°C water bath. Thereafter, Alg was added to GelMA solution (the molar ratio of GelMA/Alg = 2:1) under atmospheric pressure and stirred in the dark for 20 min to form a homogeneous pre-hydrogel solution for 3D printing. The GelMA/Alg pre-hydrogel was transferred into a cylinder and installed into a 3D printer (Bioscaffolder 3.1; GeSiM, Germany). The printing parameters were 0.1–0.2 kPa for air pressure, 0.15 mm for fiber spacing and height, 10 mm/s for the printing speed, 50–60°C for the material barrel, and −20°C for the print platform. The angle between scaffold struts was 60°. The stimulators mixed into the material were 200 μM PA and 50 μM PRO. The 3D-printed scaffold was then put into the UV-light crosslinker for about 5 min and immersed in 1 mol/L of calcium chloride for further crosslinking and storage.[22,23]

2.4. Morphological examination with scanning electron microscopy

The appearance of the scaffolds, such as strands, pore size, and cross-section morphologies, was examined through a scanning electron microscope (SEM; ZEISS SUPRA®55; Carl Zeiss, Germany). Before SEM examination, the scaffolds were lyophilized in a freeze-dryer (BYK-025_TY3341; Beijing Boyikang Experimental Instrument Co. Ltd., China) for 24 h, and then coated with gold via a sputter coater.

2.5. Rheological testing

Rheological tests were performed with the ink on a rheometer (TA Instrument, Austria). The stage temperature was controlled between 15 and 40°C. The ink was loaded onto the stage, and mineral oil was used to prevent dehydration. The temperature sweep was carried out at 0.5°C/min and 1% strain.

2.6. Fourier-transform infrared spectroscopy

Fourier-transform infrared (FTIR) spectrometry (BRUKER VERTEX 70; Bruker, USA) was used to confirm the successful synthesis of the hydrogel.

2.7. Measurement of mechanical properties

The mechanical properties were evaluated via uniaxial compression test. After equilibration in deionized water, the scaffolds (14 × 14 × 3.5 mm) were measured on the tester (Instron 5697; Instron, USA). The crosshead speed was set at 10 mm/min.

2.8. Histological analyses

The tissues were collected and fixed in 4% paraformaldehyde for 24 h, dehydrated through graded ethanol, and embedded in paraffin. Thereafter, 5-μm-thick sections were stained with hematoxylin and eosin staining. For immunostaining, 3% peroxide was used to block endogenous peroxidase activity for 10 min at room temperature. Non-specific binding was blocked in phosphate-buffered saline (PBS) with 5% bovine serum albumin for 1 h at room temperature, followed by incubation with primary antibody (zona pellucida glycoprotein 3 [ZP3]) diluted in blocking solution (1:100) overnight at 4°C. After fully washing with PBS, the sections were incubated with the secondary antibody diluted in blocking solution for 1 h and detected with fresh diaminobenzidine solution; sections were counterstained with hematoxylin. Finally, the slides were photographed using an Olympus microscope (IX73P1F; Olympus, Japan).

2.9. PRO release assay

For the release assay, PRO was dissolved in the saline and PBS. The concentrations of the standard curve were 0, 3.125, 6.25, 12,5, 25, 50, and 100 μM, respectively. Scaffolds containing PRO were cut into 10 × 10 mm^2 and added into a 6-well plate with 5 mL saline and PBS, respectively. The drug release test was performed in a constant temperature shaker at 37°C with a rotational speed of 150 rpm. Approximately, 200 μL medium was removed at indicated time points, and the corresponding released medium of the same volume was added. The concentration of PRO in each sample was analyzed using a UV spectrophotometer (UV-8000, China) at 320 nm.[24] The cumulative drug release at different time points was calculated according to the standard curve.

2.10. Granulosa cell isolation and culture

The collection of ovarian granulosa cells was performed as described previously.[25] Briefly, 25-day-old female GFP mice were treated with pregnant mare serum gonadotropin (5 IU; ProSpec, Israel) for 48 h. Ovaries were removed and dissected from the oviducts and fat with a dissecting microscope. Granulosa cells were obtained from the ovarian tissue by follicular puncture and placed in PBS. The cell suspension was filtered with a 70 μm mesh sieve to remove oocytes and centrifuged at 1000 × *g* for 3 min.

Granulosa cells were cultured in DMEM/F12 medium complemented with 10% fetal bovine serum, 100 IU/mL penicillin, and 100 mg/mL streptomycin sulfate shortly for use. These granulosa cells were then seeded into the scaffold in 24-well plates for 7 days. The morphological change of the granulosa cells and scaffold was observed under a fluorescence microscope on days 1 and 7.

2.11. Transplantation

Ovaries from neonatal C57BL/6J mice were collected on day 3, as described above. The scaffolds were cut into proper size for implantation and rinsed with saline for 5 min. The recipient C57BL/6 mice (8–10 weeks) were weighed and anesthetized with avertin intraperitoneally. For kidney capsule transplantation, a longitudinal skin incision was made on the dorsum to expose the position of the kidney. A pair of forceps was used to hold the kidney out of the body; two small forceps were then used to split the capsule. Scaffolds with ovarian tissue were inserted into the capsule. For subcutaneous ectopic transplantation, the scaffolds containing ovarian tissue with or without stimulators were transplanted subcutaneously at the abdominal region of the recipient. Finally, sutures were used to close the incision. Due to the deficiency of growth hormone in ovariectomized recipient mice, the follicle stimulating hormone (FSH; 1 IU per day) was administrated through intraperitoneal injection to promote follicle growth. Three repeats of the experiment were carried out.

2.12. Statistical analysis

Data are presented as the mean ± Structural Equation Model (SEM). The statistical significance was assessed by a two-tailed Student's *t*-test. A p-value < 0.05 was considered statistically significant in this study.

3. Results

3.1. Preparation of scaffold materials and appearance of the 3D-printed porous scaffolds

Figure 1A illustrates the 3D printing process of the GelMA/Alg composite scaffold. The GelMA, containing unsaturated double bonds, can be efficiently crosslinked by UV light, while Alg can form an ionic crosslinking network through its strong interaction with divalent ions. This combination could enhance the construction of a high-strength GelMA/Alg composite hydrogel with double crosslinking networks. Moreover, the RGD motifs in the backbone of GelMA were beneficial for improving the biocompatibility of GelMA-based hydrogels; Alg's ability to adjust viscosity exhibits an outstanding adaptability for printing. Thus, the composite GelMA/Alg (2:1 in molar ratio) ink was ready for 3D printing; UV and ionic crosslinking were applied to solidify the 3D-printed GelMA/Alg hydrogel scaffolds. The printing process is displayed in Figure 1B and Video S1 (see Supplementary Information). The final shape of the printed scaffold after double crosslinking is featured in Figure 1C–F. The freeze-dried 3D scaffold microstructure displays a network of interconnected pores, and each pore size of the scaffold was 200 ± 50 μm (Figure 1G–I).

3.2. Gelatin/alginate-based scaffolds exhibit applicable mechanical properties

To meet the extrusion requirements of bioink, we generated a GelMA/Alg complex with optimized rheological properties to align with the pressure extrusion of a 3D printer (Figure 2A–D). The GelMA/Alg ink displays typical shear-thinning behaviors, and the viscosity can be adjusted by regulating the temperature in the range of 20–40°C, which is advantageous for extrusion printing. Characteristic absorption peaks at 819, 1031, and 1418 cm^{-1} for Alg, and 1242, 1336, and 1536 cm^{-1} for gelatin confirm the successful fabrication of hydrogel scaffold after double crosslinking (Figure 2E). At room temperature, 90% compression deformation was achieved for all wet-state supports. The scaffold exhibited good mechanical properties. The compression strength was about 3.3 MPa, with 400 kPa modulus, indicating that the scaffold was soft and elastic (Figure 2F).

3.3. Survival of ovarian granulosa cells *in vitro*

The process of isolating mice ovarian granulosa cells and cultivating them in a scaffold is illustrated in Figure 3A. To test the compatibility of the scaffold with ovarian cells, we chose granulosa cells dissected from GFP transgenic mice, which could be observed easily under a fluorescent microscope. It is demonstrated that the granulosa cells can adhere to the struts and maintain the basic cell morphology by day 1 (Figure 3B and D); an increase in interactions between the granulosa cells and the scaffold was observed after 7 days of culture (Figure 3C). Notable, the scaffold partially degraded over time, but the granulosa cells continued to grow in the struts, indicating that the scaffolds effectively support the survival of ovarian granulosa cells (Figure 3E).

3.4. Biocompatibility of the scaffolds for follicles under the kidney capsule

Although both gelatin and Alg are approved by the Food and Drug Administration (FDA, USA) and the National Medical Products Administration (NMPA, China) for clinical tissue engineering,[26,27] their biocompatibility for combined use for follicle development remains unclear.

The primordial follicle consists of a dormant oocyte and a single layer of pre-granulosa cells, which is at the initial stage of folliculogenesis and determines the duration of female reproduction.[28] In rodents, primordial follicles are

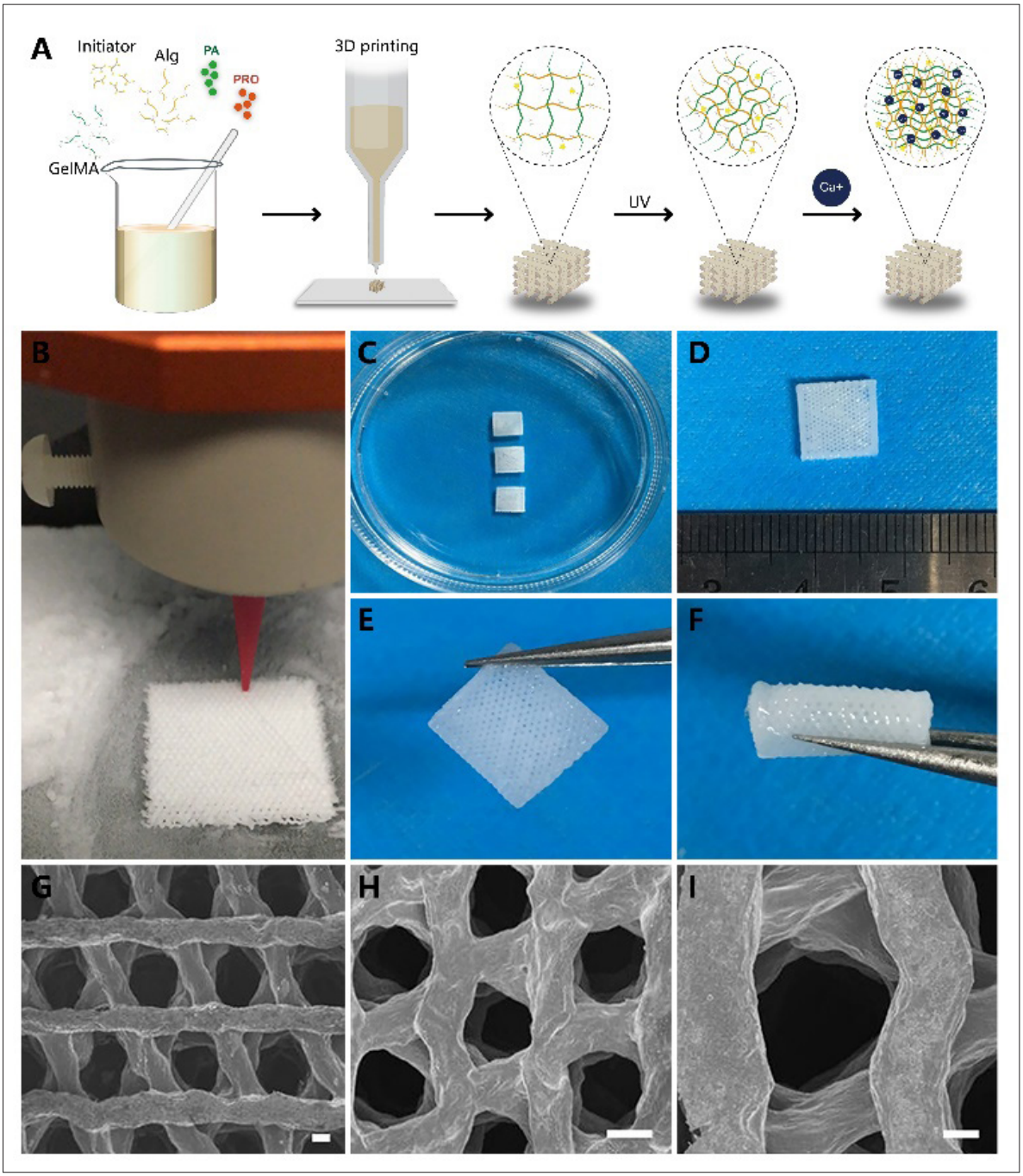

Figure 1. (A) Preparation of scaffold materials and the morphology of 3D-printed porous scaffolds. Te 3D printing process of the GelMA/Alg composite scaffold. (B) Te process of 3D printing on cryo-stage. (C–F) Appearance of scaffolds with proper elasticity. Appearance of the scaffolds (C), size of the scaffolds (D), side of the scaffolds (E), side of the scaffolds (F). (G–I) Observation of scaffold morphology via scanning electron microscopy is shown as magnification 40X (G), 50X (H), 100X (I), respectively. Scale bars: 100 μm (G, I), 200 μm (H). Abbreviations: Alg, alginate; GelMA, gelatin methacryloyl; UV, ultraviolet.

formed at about 19.5 days post coitum and re-assembled in the ovary until day 3 post parturition.[29] To validate the activation ability of PRO and PA, we selected the day 3 neonatal ovary as the model.

To validate scaffold biocompatibility for follicle development, the dissected day 3 ovarian tissue was placed in the scaffold and transplanted under the renal capsule of the adult female mouse with the ovary removed

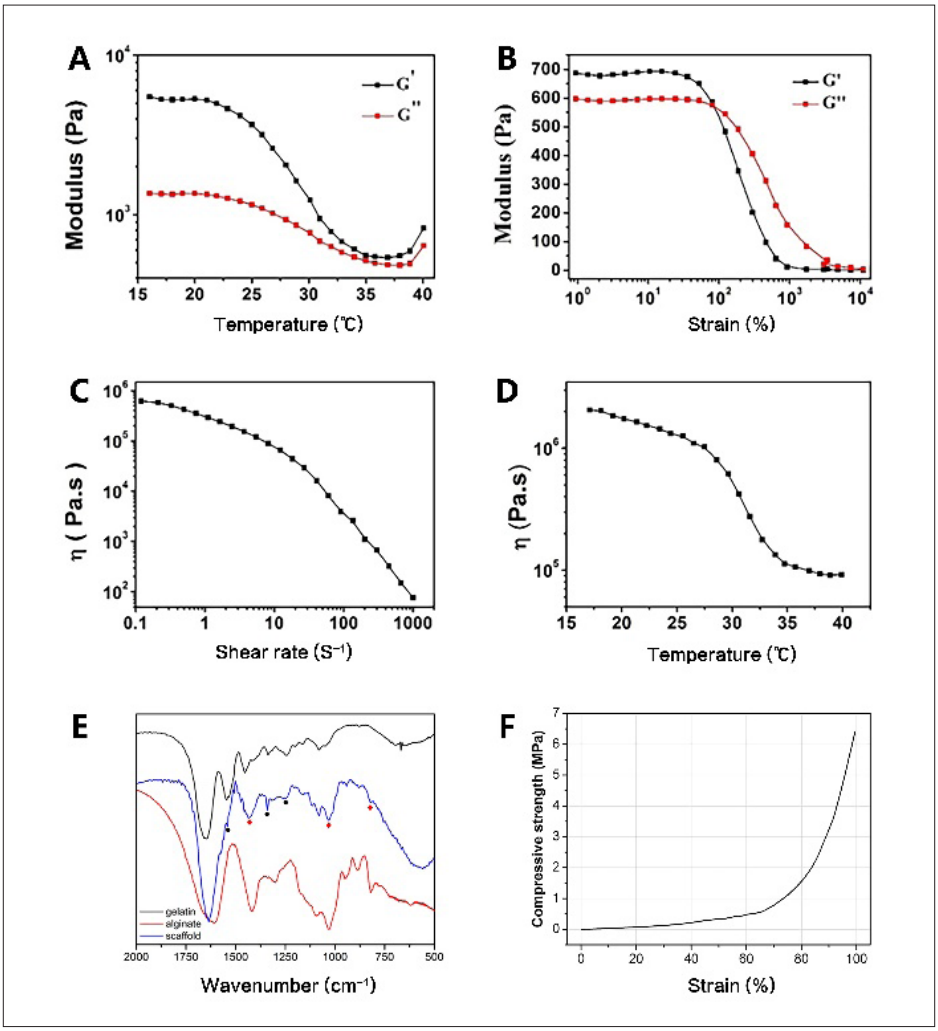

Figure 2. Mechanical properties of scaffolds. (A) Rheological properties of the scaffolds. (B) Tensile stress–strain and compressive stress–strain curves of the scaffolds. (C) Viscosity measurement of the scaffolds. (D) Result of temperature amplitude sweep test. (E) FTIR spectra. (F) Mechanical properties of the scaffolds. Abbreviations: FTIR, Fourier Transform Infrared Spectroscopy; G', elastic modulus; G'', damping modulus.

(Figure 4A–E). Results from Figure 4F and G suggested that follicle development within the scaffold proceeded normally after 1 week, with comparable morphology to the directly implanted day 3 ovarian tissue in the kidney capsule (Figure 4H and I).

3.5. Scaffold-induced sustained drug release

To activate the primordial follicles *in situ*, the ability of the scaffold to release activators locally is vital. PRO was chosen to evaluate the drug-release capabilities of the scaffold, and the concentrations of released PRO in saline and PBS were detected using a fluorescence spectrophotometer.

Standard curves of different PRO concentrations were initially plotted (Figure 5A and B). Then, at different time points, the supernatant collected from the two groups was evaluated to measure the PRO concentration. The results indicated that over time, the scaffold in saline rapidly released approximately 30% of PRO within the first hour, with a gradual increase to about 50% in 1–8 h, and then plateaued up to 96 h (Figure 5C). Similarly, the scaffolds in PBS also rapidly released 40% of the PRO in the first 4 h, slowly increasing to 50% in 4–24 h, and then also plateaued up to 96 h (Figure 5D). The scaffolds exhibited a consistent release profile in both saline and PBS, with a similar overall trend and sustained release efficiencies.

This characteristic has enabled us to develop a controlled system for realizing drug release. The PBS buffer was the primary compound of the tissue environment; the scaffold could be degraded slowly without extra stimulus, and the activators could be locally released, thereby minimizing systemic side effects.

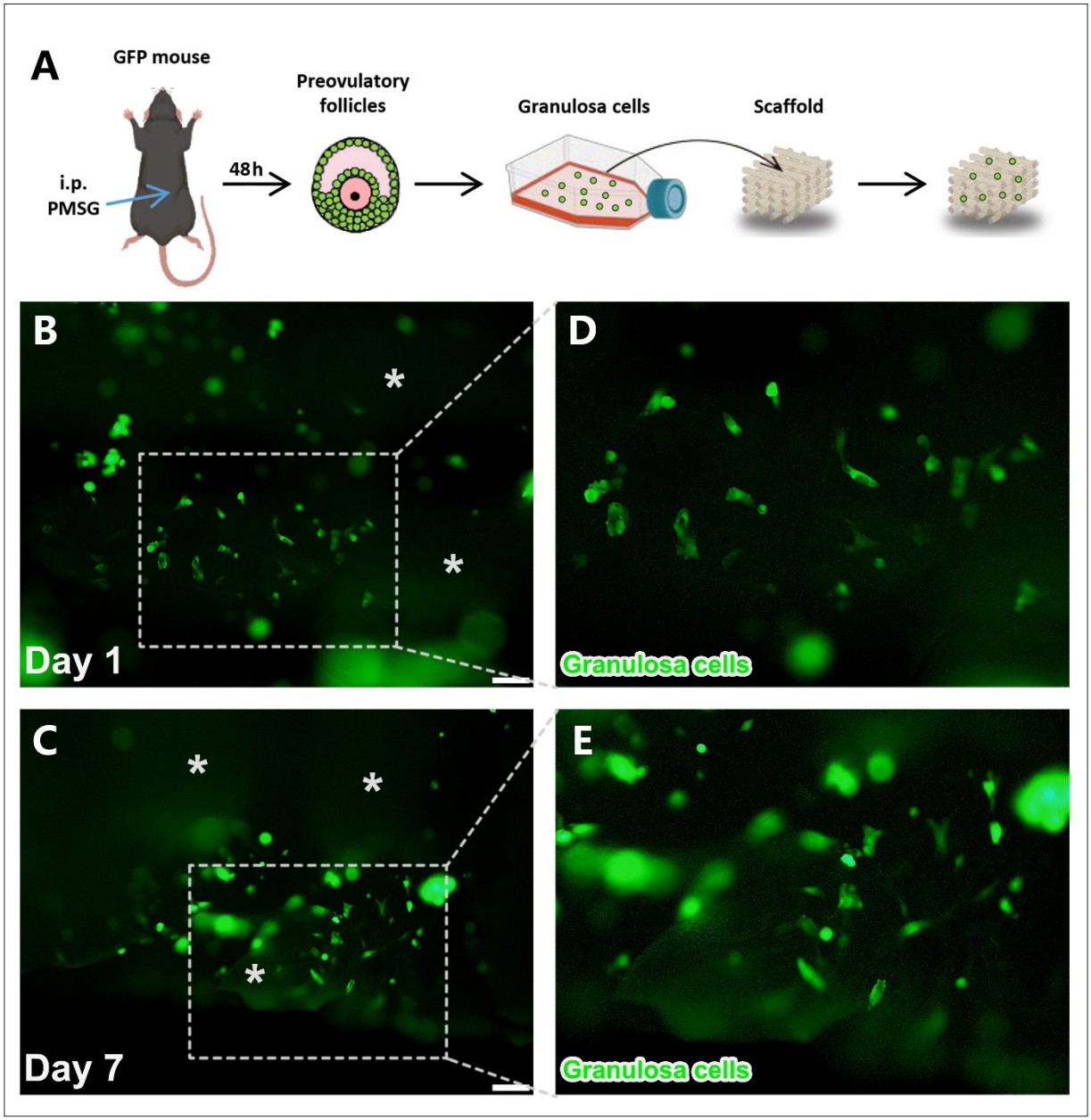

Figure 3. Ovarian granulosa cells survived in the scaffolds and interacted with struts *in vitro*. (A) The process of mouse ovarian granulosa cell isolation and implantation into the scaffold. (B and D) Fluorescence imaging of granulosa cells isolated from GFP transgenic mouse on the struts from day 1 of culture. (C and E) After 7 days of culture, the granulosa cells survived on the struts. * indicates the struts. Scale bar: 100 μm. Abbreviations: GFP, green fluorescent protein; i.p., intraperitoneal injection; PMSG, pregnant mare serum gonadotropin.

3.6. Dormant ovarian follicle activation and development in ectopic subcutaneous tissue

To ensure the practical use of an implanted artificial ovary, we tested if the scaffolds could support the activation and development of the primordial follicles when injected subcutaneously. We implanted the activated or inactivated ovary–scaffold complex into the abdominal subcutaneous pocket (Figure 6A). After FSH treatment in both activation and inactivation groups for 1 week, the primordial follicles in the activation group displayed obvious growing follicular morphological features, which were not observed in the inactivated group (Figure 6B). There is a significant increase in growing follicles in the activated group compared to the inactivated group (Figure 6C). Although few follicles could be observed in the inactivated group, there were no multiple layers of cuboidal granulosa cells,

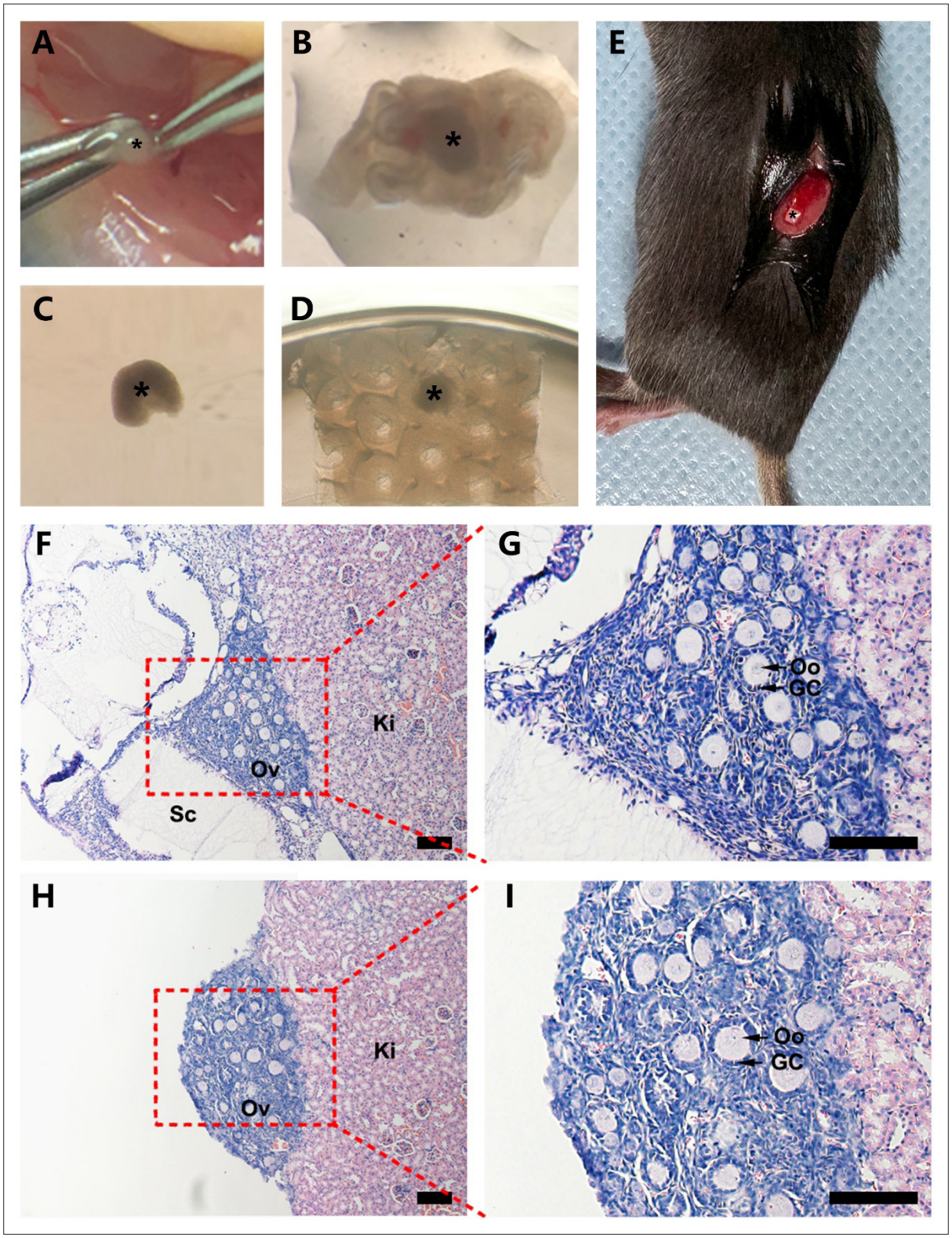

Figure 4. Biocompatibility test for the scaffolds under the kidney capsule. (A–E) Day 3 mouse ovary dissection, which was transferred to the scaffold, and then transplanted under the dorsal membrane of the kidney. (F and H) H&E section staining of kidney and ovary with scaffolds after transplantation for 1 week. (G and I) Enlarged morphology of ovary tissue grafted into the kidney capsule. Arrows indicated the ovary. Abbreviations: GC, granulosa cells; H&E, hematoxylin-eosin staining; Ki, kidney; Oo, oocyte; Ov, ovary; Sc, scaffold. Scale bars: 250 μm.

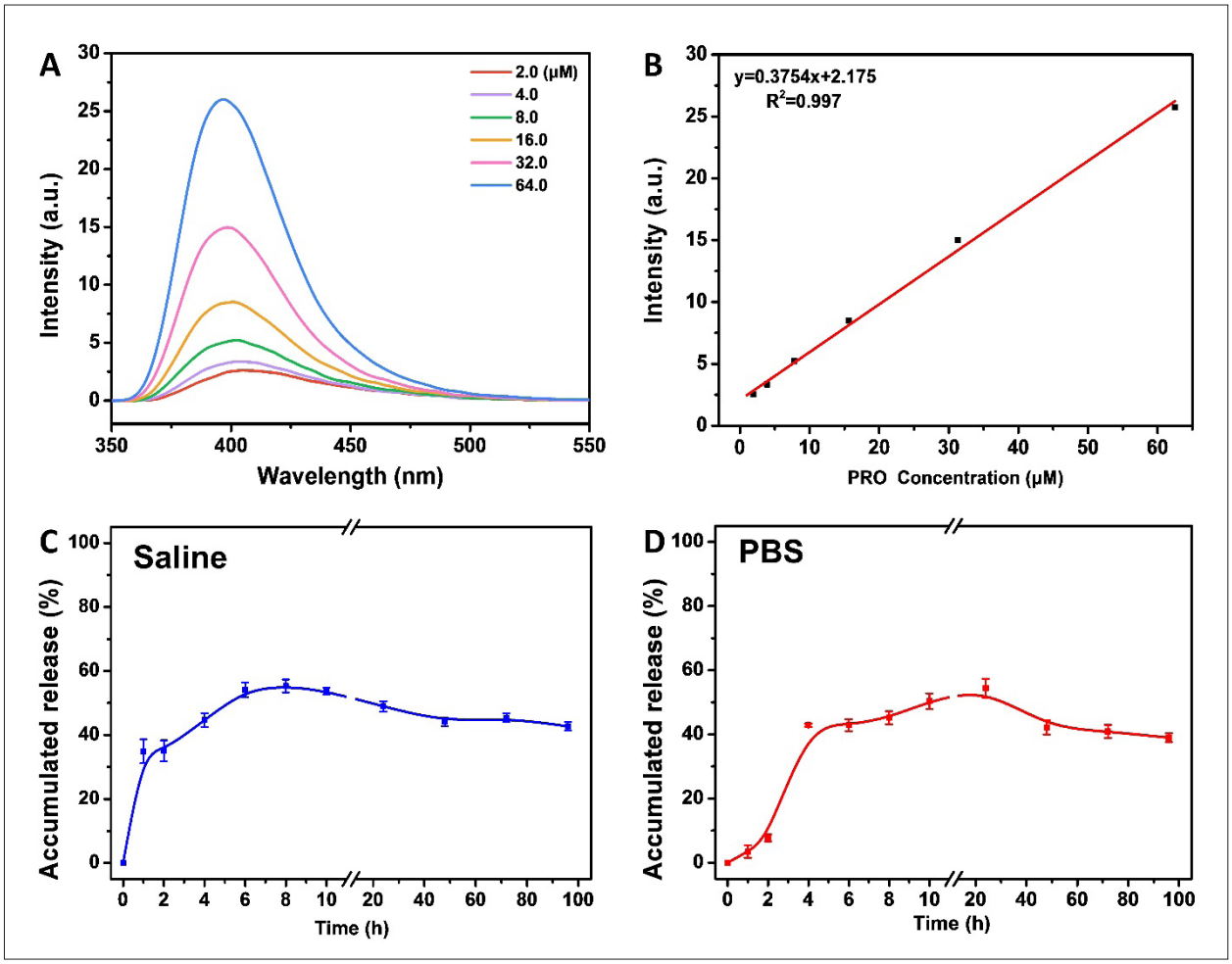

Figure 5. Sustained drug release in scaffolds. Propranolol (PRO) has a maximum emission spectrum at an excitation wavelength of 320 nm. (A) Fluorescence spectrum of different PRO concentrations. According to the maximum emission spectrum of different concentrations of PRO in Figure A, a (B) standard curve plotted based on (A). (C and D) Cumulative sustained release of the scaffold containing PRO in saline (C) and PBS (D), respectively ($n = 3$). The accumulated release refers to the amount of PRO in the scaffold. Abbreviation: PBS, phosphate-buffered saline.

which is essential during follicle development. These results were further confirmed by specific immunofluorescent staining of growing follicle biomarker ZP3. In addition, an abundance of growing follicles with zona pellucida shape and more granular cell layers were noticeable in the activated group, while the inactivated group lacked distinct ovarian and follicle morphological features (Figure 6D).

4. Discussion

Ovarian dysfunction would cause abnormalities in oogenesis, folliculogenesis, and ovulation, leading to infertility and endocrine disorders. Among them, primary ovarian insufficiency (POI) refers to the loss of ovarian functional follicles in women before the age of 40.[30] For patients with POI who have fertility needs, the most effective treatment is assisted reproductive technology. Clinical practice has found that the development potential of oocytes matured *in vitro* is poor, the abortion rate of embryo formation is relatively high, and there are no recognized effective improvement measures. Therefore, in this study, we introduced a strategy for the ectopic activation and development of primordial follicles *in vivo*, utilizing a well-designed scaffold printed from Alg and gelatin, integrated with activators.

Several materials have been utilized for printing 3D ovarian models, such as Alg, fibrin, and collagen.[14] In this study, we selected two widely used biomaterials in bioengineering that have excellent biocompatibility. Apart from materials, the crosslinking method is also critical to ensuring the function of the ovarian model. To date, the crosslinking methods for hydrogel include both chemical and physical methods.[31] Chemical methods refer to gels

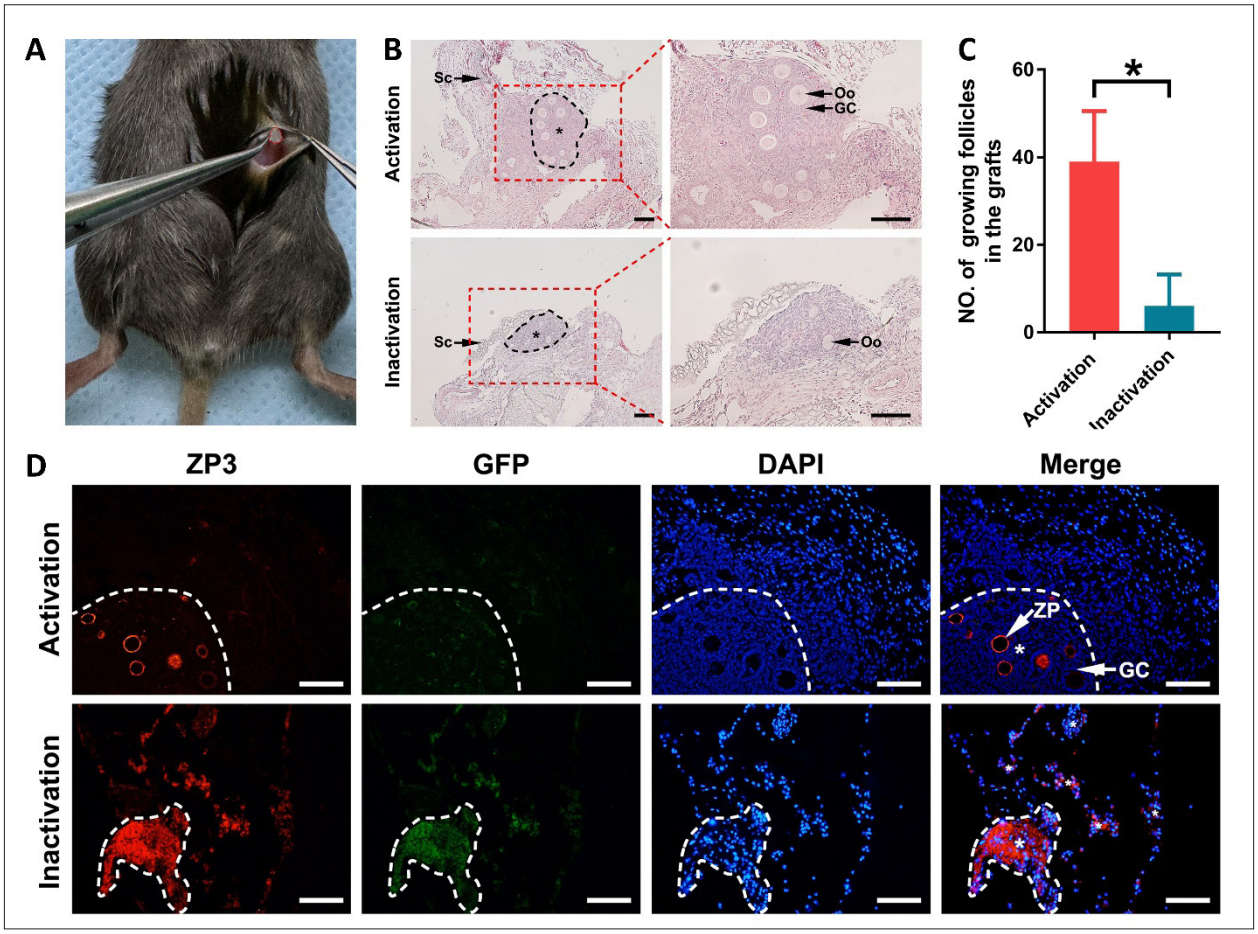

Figure 6. Dormant ovarian follicles were activated and developed within the ectopic subcutaneous tissue. (A) Schematic diagram of subcutaneous ectopic transplantation with scaffolds containing activators and day 3 ovary. (B) Morphological comparison of activated or inactivated primordial follicles. (C) Quantitative analysis was performed by counting the growing follicles in the grafts (n = 3). * indicates a significant difference (P=0.0137). (D) Immunofluorescent detection of growing follicle marker ZP3. The asterisk indicated the grafted ovary tissue. Abbreviations: GC, granulosa cells; Oo, Oocyte; Sc, scaffold; ZP, zona pellucida. Scale bars: 200 μm (B); 250 μm (D).

formed through the action of specific compounds or ions, such as Alg and DNA gel; physical methods are based on networks triggered by specific light wavelength or temperature changes, such as methylacrylamide-modified gelatin used in this study.[32] Therefore, in this study, by optimizing the ratio of gelatin to Alg, precisely controlling the 3D printer parameters, and combining the chemical and physical crosslinking methods, we have successfully obtained scaffolds with high porosity, uniform structure, and good mechanical stability. Furthermore, the results of co-culturing with granulosa cells and renal subcapsular transplantation indicate that the cells and ovarian tissues can survive and further develop in the scaffold, suggesting that the scaffold has good biocompatibility.

For primordial follicle activation, we selected a relatively mature activator combination, PA and PRO, which have been reported to activate the primordial follicle via the mTOR signaling pathway.[33] To date, studies related to primordial follicle activation have predominantly focused on signaling pathways. The use of the knockout mice model has revealed several signaling pathways in oocytes that contribute to the regulation of follicle activation. For example, the PI3K-PTEN-AKT-FOXO3 pathway is one of the most extensively studied.[34–36] Additionally, the downstream signal, mTOR, is regulated by the activation of AKT.[37,38] Currently, a variety of related activators and inhibitors have been used in clinical practice for the treatment of POI, such as the combination of mTOR and PI3K activators,[33] or mTOR and AKT activators.[39] Moreover, there are other alternative options for activating primordial follicles *in vitro*; further investigation is warranted to determine whether these options could still activate primordial follicles when incorporated into a scaffold.

The results of the release assay revealed that activators preloaded in the scaffolds could be gradually released in both PBS and saline, providing a more controlled system compared to the traditional in vitro activation process, which requires several hours of *in vitro* activation. This approach shortens patients' waiting time and reduces the adverse effects of prolonged exposure on follicles and oocytes when cultured *in vitro*. Furthermore, the ectopic activation model established here sheds light on future clinical applications and enables the growth of follicles through simple surgery and subcutaneous ectopic transplantation. Subcutaneous transplantation also simplifies the further handling of growing follicles, allowing for direct monitoring using ultrasonic techniques or the isolation of mature follicles for in vitro fertilization procedures.

By combining optimized biomaterials and 3D printing technology, along with the incorporation of primordial follicle activators, the future development of an artificial prosthetic ovary is on the horizon. This progress is expected to help alleviate endocrine disorders and even facilitate oocyte maturation.

5. Conclusion

We introduced a novel approach to developing a bioactive scaffold that could activate primordial ovarian follicles and facilitate their development into growing follicles in subcutaneous implantation sites. This study, for the first time, demonstrates the use of biostimulators released from biodegradable 3D scaffolds to more readily activate the primordial follicles ectopically. However, some technical challenges still need to be addressed. For example, it would be advantageous to implement *in vivo* imaging techniques for real-time monitoring of follicular development in the scaffold and develop a vascular system to supply nutrients to the scaffold.

Acknowledgments

None.

Funding

This study was supported by the National Natural Science Foundation of China (82301907), Guangdong Basic and Applied Basic Research Foundation (2024A1515010059 and 2024A1515030279), Shenzhen Medical Research Fund (B2404004), Shenzhen Science and Technology Program (JCYJ20220818101218040, JCYJ20220818103608017, JCYJ20220818103607015, JCYJ20220818102811025, JSGGKQTD20210831174330015), Shenzhen Key Laboratory of Metabolic Health (Grant No. ZDSYS20210427152400001), Sino-European Center of Biomedicine and Health.

Conflict of interest

The authors declare there is no conflict of interest.

Author contributions

Conceptualization: Jian V. Zhang, Changshun Ruan, Pei-Gen Ren
Data curation: Yali Yang, Mingming Wu
Formal analysis: Huashan Zhao, Zhonglin Xiao
Methodology: Yali Yang, Li Xue, Meiyue Wang, Jie Chen
Investigation: Jian V. Zhang, Tianxia Xiao
Writing – original draft: Yali Yang, Huashan Zhao
Writing – review & editing: Feifei Du, Li Ge, Pinpin Wang

Ethics approval and consent to participate

The animal experiments in this study were approved by the Institutional Animal Care and Use Committee of the Shenzhen Institutes of Advanced Technology, Chinese Academy of Sciences. All applicable guidelines and protocols for the care and use of animals were followed.

Consent for publication

Not applicable.

Availability of data

Data is available from the corresponding author upon reasonable request.

Supporting information

Video S1: The process of 3D printing on cryo-stage.

References

1. Liu CM, Ding LJ, Li JY, Dai JW, Sun HX. Advances in the study of ovarian dysfunction with aging. *Hereditas.* 2019;41(9):816-826.
doi: 10.16288/j.yczz.19-134

2. Harada M. Cellular senescence in the pathogenesis of ovarian dysfunction. *J Obstet Gynaecol Res.* 2024;50(5):800-808.
doi: 10.1111/jog.15918

3. Zhang T, He M, Zhang J, et al. Mechanisms of primordial follicle activation and new pregnancy opportunity for premature ovarian failure patients. *Front Physiol.* 2023;14:1113684.
doi: 10.3389/fphys.2023.1113684

4. Ford EA, Beckett EL, Roman SD, McLaughlin EA, Sutherland JM. Advances in human primordial follicle activation and premature ovarian insufficiency. *Reproduction.* 2020;159(1):R15-R29.
doi: 10.1530/rep-19-0201

5. Luyckx V, Dolmans MM, Vanacker J, et al. A new step toward the artificial ovary: survival and proliferation of isolated murine follicles after autologous transplantation in a fibrin scaffold. *Fertil Steril.* 2014;101(4):1149-1156. doi: 10.1016/j.fertnstert.2013.12.025

6. Vanacker J, Luyckx V, Dolmans MM, et al. Transplantation of an alginate-matrigel matrix containing isolated ovarian cells: first step in developing a biodegradable scaffold to transplant isolated preantral follicles and ovarian cells. *Biomaterials.* 2012;33(26):6079-6085. doi: 10.1016/j.biomaterials.2012.05.015

7. Shikanov A, Xu M, Woodruff TK, Shea LD. Interpenetrating fibrin-alginate matrices for in vitro ovarian follicle development. *Biomaterials.* 2009;30(29):5476-5485. doi: 10.1016/j.biomaterials.2009.06.054

8. Xu M, Fazleabas AT, Shikanov A, et al. In vitro oocyte maturation and preantral follicle culture from the luteal-phase baboon ovary produce mature oocytes. *Biol Reprod.* 2011;84(4):689-697. doi: 10.1095/biolreprod.110.088674

9. Kreeger PK, Deck JW, Woodruff TK, Shea LD. The in vitro regulation of ovarian follicle development using alginate-extracellular matrix gels. *Biomaterials.* 2006;27(5):714-723. doi: 10.1016/j.biomaterials.2005.06.016

10. Shikanov A, Zhang Z, Xu M, et al. Fibrin encapsulation and vascular endothelial growth factor delivery promotes ovarian graft survival in mice. *Tissue Eng Part A.* 2011;17(23-24):3095-3104. doi: 10.1089/ten.TEA.2011.0204

11. Kniazeva E, Hardy AN, Boukaidi SA, Woodruff TK, Jeruss JS, Shea LD. Primordial follicle transplantation within designer biomaterial grafts produce live births in a mouse infertility model. *Sci Rep.* 2015;5:17709. doi: 10.1038/srep17709

12. Henning NFC, Jakus AE, Laronda MM. Building organs using tissue-specific microenvironments: perspectives from a bioprosthetic ovary. *Trends Biotechnol.* 2021;39(8):824-837. doi: 10.1016/j.tibtech.2021.01.008

13. Jin Z, Li Y, Yu K, et al. 3D printing of physical organ models: recent developments and challenges. *Adv Sci.* 2021;8(17):e2101394. doi: 10.1002/advs.202101394

14. Nair R, Kasturi M, Mathur V, Seetharam RN, S Vasanthan K. Strategies for developing 3D printed ovarian model for restoring fertility. *Clin Transl Sci.* 2024;17(7):e13863. doi: 10.1111/cts.13863

15. Pennarossa G, Arcuri S, De Iorio T, Gandolfi F, Brevini TAL. Current advances in 3D tissue and organ reconstruction. *Int J Mol Sci.* 2021;22(2):830. doi: 10.3390/ijms22020830

16. Wu T, Gao YY, Su J, et al. Three-dimensional bioprinting of artificial ovaries by an extrusion-based method using gelatin-methacryloyl bioink. *Climacteric.* 2022;25(2): 170-178. doi: 10.1080/13697137.2021.1921726

17. Laronda MM, Rutz AL, Xiao S, et al. A bioprosthetic ovary created using 3D printed microporous scaffolds restores ovarian function in sterilized mice. *Nat Commun.* 2017;8:15261. doi: 10.1038/ncomms15261

18. Aydin S, Yaşlı M, Yildiz Ş, Urman B. Advancements in three-dimensional bioprinting for reproductive medicine: a systematic review. *Reprod Biomed Online.* 2024;49(4):104273. doi: 10.1016/j.rbmo.2024.104273

19. Gandolfi F, Ghiringhelli M, Brevini TAL. Bioengineering the ovary to preserve and reestablish female fertility. *Anim Reprod.* 2020;16(1):45-51. doi: 10.21451/1984-3143-ar2018-0099

20. Zivari-Ghader T, Dolati S, Mehdizadeh A, Davaran S, Rashidi MR, Yousefi M. Recent scaffold-based tissue engineering approaches in premature ovarian failure treatment. *J Tissue Eng Regen Med.* 2022;16(7):605-620. doi: 10.1002/term.3306

21. Gao F, Xu Z, Liang Q, et al. Osteochondral regeneration with 3D-printed biodegradable high-strength supramolecular polymer reinforced-gelatin hydrogel scaffolds. *Adv Sci.* 2019;6(15):1900867. doi: 10.1002/advs.201900867

22. Gao F, Xu ZY, Liang QF, et al. Direct 3D printing of high strength biohybrid gradient hydrogel scaffolds for efficient repair of osteochondral defect. *Adv Funct Mater.* 2018;28(13):1706644. doi: 10.1002/adfm.201706644

23. Zhai X, Ruan C, Ma Y, et al. 3D-bioprinted osteoblast-Laden nanocomposite hydrogel constructs with induced microenvironments promote cell viability, differentiation, and osteogenesis both in vitro and in vivo. *Adv Sci.* 2018;5(3):1700550. doi: 10.1002/advs.201700550

24. Sahoo J, Murthy PN, Biswal S, Sahoo SK, Mahapatra AK. Comparative study of propranolol hydrochloride release from matrix tablets with KollidonSR or hydroxy propyl methyl cellulose. *AAPS PharmSciTech.* 2008;9(2):577-582. doi: 10.1208/s12249-008-9092-2

25. Yang YL, Sun LF, Yu Y, et al. Deficiency of Gpr1 improves steroid hormone abnormality in hyperandrogenized mice. *Reprod Biol Endocrinol.* 2018;16(1):50. doi: 10.1186/s12958-018-0363-9

26. Sosnik A. Alginate particles as platform for drug delivery by the oral route: state-of-the-art. *ISRN Pharm.* 2014;2014:926157. doi: 10.1155/2014/926157

27. Jaipan P, Nguyen A, Narayan RJ. Gelatin-based hydrogels for biomedical applications. *MRS Commun.* 2017;7(3):416-426. doi: 10.1557/mrc.2017.92

28. Pepling ME. From primordial germ cell to primordial follicle: mammalian female germ cell development. *Genesis*. 2006;44(12):622-632.
doi: 10.1002/dvg.20258

29. O'Connell JM, Pepling ME. Primordial follicle formation – some assembly required. *Curr Opin Endocr Metab Res.* 2021;18;118-127.
doi: 10.1016/j.coemr.2021.03.005

30. Wesevich V, Kellen AN, Pal L. Recent advances in understanding primary ovarian insufficiency. *F1000Res*. 2020;9:F1000 Faculty Rev-1101.
doi: 10.12688/f1000research.26423.1

31. Gill EL, Li X, Birch MA, Huang YYS. Multi-length scale bioprinting towards simulating microenvironmental cues. *Biodes Manuf.* 2018;1(2):77-88.
doi: 10.1007/s42242-018-0014-1

32. Xu C. Freeform vertical and horizontal fabrication of alginate-based vascular-like tubular constructs using inkjetting. *J Manuf Sci Eng.* 2014;136(6):061020.

33. Sun X, Su Y, He Y, et al. New strategy for in vitro activation of primordial follicles with mTOR and PI3K stimulators. *Cell Cycle*. 2015;14(5):721-731.
doi: 10.1080/15384101.2014.995496

34. Castrillon DH, Miao L, Kollipara R, Horner JW, DePinho RA. Suppression of ovarian follicle activation in mice by the transcription factor Foxo3a. *Science.* 2003;301(5630):215-218.
doi: 10.1126/science.1086336

35. Liu L, Rajareddy S, Reddy P, et al. Infertility caused by retardation of follicular development in mice with oocyte-specific expression of Foxo3a. *Development.* 2007;134(1):199-209.
doi: 10.1242/dev.02667

36. Reddy P, Liu L, Adhikari D, et al. Oocyte-specific deletion of Pten causes premature activation of the primordial follicle pool. *Science.* 2008;319(5863):611-613.
doi: 10.1126/science.1152257

37. Adhikari D, Flohr G, Gorre N, et al. Disruption of Tsc2 in oocytes leads to overactivation of the entire pool of primordial follicles. *Mol Hum Reprod.* 2009;15(12):765-770.
doi: 10.1093/molehr/gap092

38. Adhikari D, Zheng W, Shen Y, et al. Tsc/mTORC1 signaling in oocytes governs the quiescence and activation of primordial follicles. *Hum Mol Genet.* 2010;19(3):397-410.
doi: 10.1093/hmg/ddp483

39. Cheng Y, Kim J, Li XX, Hsueh AJ. Promotion of ovarian follicle growth following mTOR activation: synergistic effects of AKT stimulators. *PLoS One.* 2015; 10(2):e0117769.
doi: 10.1371/journal.pone.0117769